Al-Neshawy, F; Puttonen, J

Determining the Location of Steel Reinforcement in Thick Concrete Walls by Non-Destructive Inspection

Published in:
Nordic Concrete Research

DOI:
10.2478/ncr-2023-0010

Published: 01/12/2023

Document Version
Publisher's PDF, also known as Version of record

Nordic Concrete Research – Publ. No. NCR 69 – ISSUE 2/ 2023 – Article 4, pp. 55-71

ISSN online 2545-2819
ISSN print 0800-6377

DOI: 10.2478/ncr-2023-0010

Received: Sept. 28, 2023
Revision received: Nov. 22, 2023
Accepted: Nov. 28, 2023

Determining the Location of Steel Reinforcement in Thick Concrete Walls by Non-Destructive Inspection

Fahim Al-Neshawy
D.Sc. (Tech.), Staff Scientist
Aalto University School of Engineering
Rakentajanaukio 4 A, 02150 Espoo, Finland
fahim.al-neshawy@aalto.fi

Jari Puttonen
Professor
Aalto University School of Engineering
Rakentajanaukio 4 A, 02150 Espoo, Finland
e-mail: jari.puttonen@aalto.fi

ABSTRACT

Concrete cover is the thickness of the concrete layer that protects the reinforcing steel bars (rebar) within a reinforced concrete structure. It acts as a barrier against external elements such as moisture, chemicals, and environmental factors, safeguarding the rebar from corrosion. Concrete cover measurement is performed by using various nondestructive tests such as GPS (Ground Penetrating Radar), electromagnetic test and ultrasonic. The main benefit of the concrete cover thickness measurement is to explain the causes of corrosion and identify areas that have the capability to corrode faster.

This paper discusses the possibilities to measure the concrete cover depth and determine the location of steel bars of a thick-walled concrete structure by using different nondestructive testing methods. The methods studied are a concrete cover meter, Ground Penetrating Radar, which is based on propagation radar waves in concrete, and Ultrasonic Pulse Echo tomography based on stress waves produced by ultrasonic pulses. The paper demonstrates the use of these methods for in-situ measurements on a thick-walled reinforced concrete structure. The concrete cover depth and the location for the reinforcement bars received by different methods are compared and the strong and weak points of the methods are discussed.

The results indicate that the concrete cover meter is suitable for measuring the thickness of concrete cover, while the Ground Penetrating Radar and the Ultrasonic Pulse Echo device were able to identify and locate the reinforcement bars position in the concrete structure.

Key words: Concrete, reinforcement, detection, non-destructive testing, radar, ultrasonic.

1. INTRODUCTION

1.1 Electromagnetic methods for detection of concrete reinforcement

In civil engineering, the most important electromagnetic NDT method is the eddy current (EC) method, which is typically used for reinforced concrete structures within excitation frequency range from 0.5 to 10 kHz. The eddy current method can be used not only to detect the presence of steel bars but also to determine the thickness of concrete cover, the diameter of bars, and the alloy of reinforcement based on the effect of alloy on electrical properties, or to detect steel corrosion [1]. The devices measuring the thickness of concrete cover use the eddy current principle with pulse induction as an electromagnetic measuring method.

Cover meter devices aim to measure non-destructively the thickness of concrete cover and the bar diameter in reinforced concrete structures. The presence of reinforcement in concrete can be detected by measuring and analyzing the electromagnetic field of reinforcement induced by the cover meter [2].

The operation principle of a concrete cover meter is shown in Figure 1, in which alternating current induced in the coil generates an alternating magnetic field. The presence of reinforcing steel in the magnetic field leads to the occurrence of eddy currents, which also form a magnetic field. The resulting change in coil impedance serves as a basis for determining the thickness of the concrete cover and the diameter of reinforcement bars [3].

Inspection is performed by dragging the device along the line, which detects only the bars that are perpendicular to the drag line. Therefore, in most cases, inspection involves multiple line checks in two directions forming a network. Measurement accuracy is limited if reinforcement intersects with installed grids, anchors, and other metals, concrete aggregates are magnetic, or the concrete cover is thick compared to the strength of magnetic field.

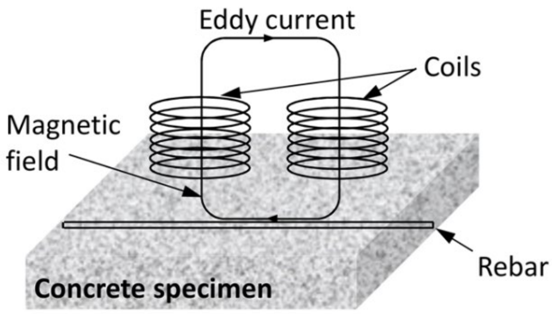

Figure 1 – Illustration of the concrete cover meter operation principle using eddy current.

Another electromagnetic method used for the detection of reinforcements and characterization of the geometry of elements of civil engineering structures is Ground-Penetrating Radar (GPR) [4]. GPRs are composed of a central unit used to set up the system and store measurement data and antennas in order to radiate electromagnetic energy. The central unit is used as an interface between the operator and the active part of the system, i.e., the antenna(s). The central unit is a micro-computer in which software is installed, enabling the system to be set up. This computer also enables storing and, in some cases, processing of the data measured.

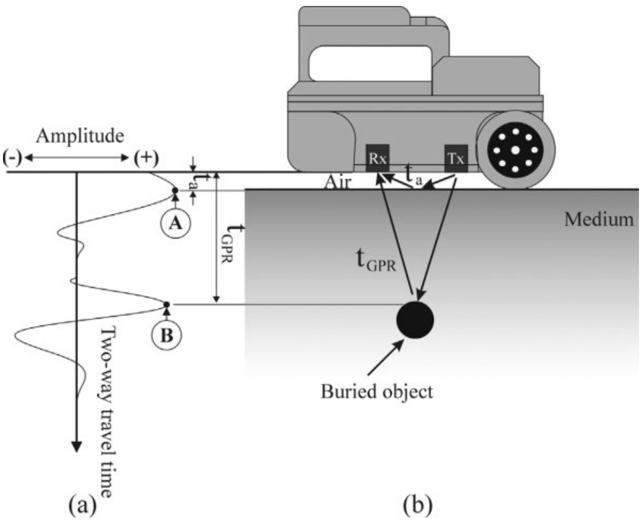

Figure 2 – Illustration of a GPR system and reflected signal from a buried object: (a) waveform, (b) reflection paths of radio wave [5] and [6].

The GPR uses antennas to transmit and receive pulses of electromagnetic energy through a medium such as ground or concrete. As the radar receives the transmitted pulses it registers "echoes" from objects based on their different electromagnetic conductivity. A simple illustration of its operation principle is shown in Figure 2. When the scanner is moved along a concrete surface, electromagnetic waves are reflected from objects beneath this surface. These objects are indicated immediately on the display.

GPR information is generally viewed as either an A-scan, B-scan (i.e., line scans) or C-scans (i.e., grid scans), as shown in Figure 3. Normally, A, B and C-scan are used for presenting the GPR data in 1, 2 and 3 dimensions, respectively. A-scan and B-scan images are vertical depth sections and provide details of the characteristics of reflected waveform's, such as estimates of signal phase, amplitude, and propagation velocity. C-scan, which explores a 3D volume, images a horizontal section for a plane at certain depth. A widely applied method for presenting the results of C-scans is horizontal slicing, in which each image is called a depth slice [7].

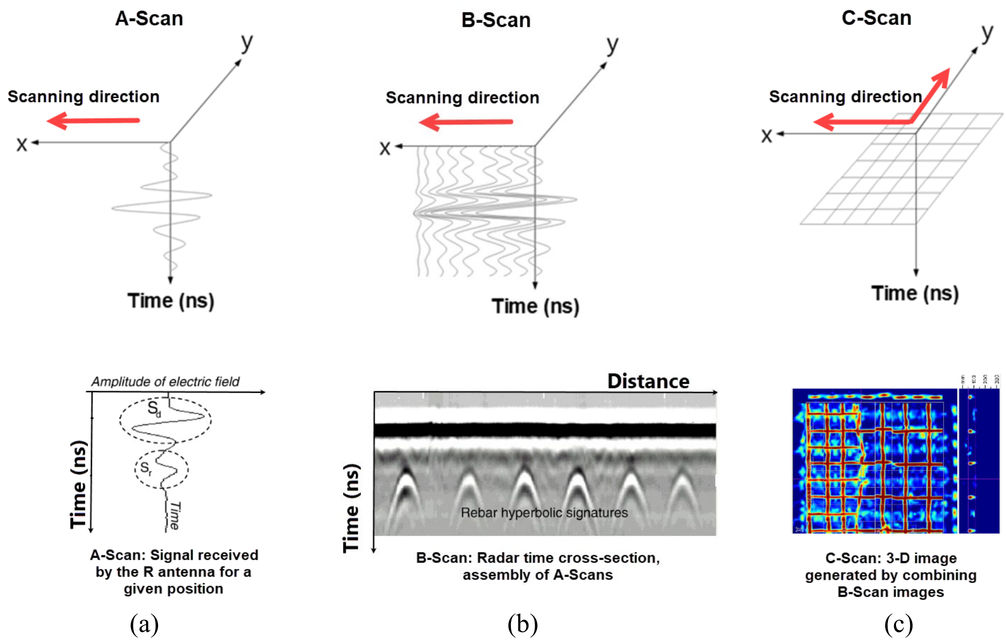

Figure 3 – Measurement principle for GPR. (a) ***A-scan*** *is the signal of the receiving antenna for a given position, (b)* ***B-scan*** *is the assembly of A-scans and (c)* ***C-Scan*** *is the 3-D image which is generated by combining simultaneous B-scan images on the XY plane* [8], [9].

1.2 Ultrasonic tomography for detecting and locating defects in concrete structures

Ultrasonic testing is a broad group of NDT techniques based on the propagation of ultrasonic waves in the object or material tested. The most used ultrasonic testing technique is the Ultrasonic Pulse Echo (UPE), wherein high-frequency sound wave beams are introduced into a test object and reflections (echoes) are returned to a receiver from internal imperfections or from geometrical surfaces. UPE methods are used for scanning embedded objects in concrete elements [10].

The basic method of ultrasonic testing is transforming a voltage pulse to an ultrasonic pulse using a transducer. Transducers consist of a piezoelectric crystal enclosed within a plastic or stainless-steel housing. The piezoelectric crystals expand when electrically charged, thus generating an acoustic wave. The signal travels through the structure reacting to its geometry and existing defects and then is either transmitted to another transducer or reflected back to the original transducer. Defects are detected if they produce a change in the acoustic impedance in the path of the ultrasonic beam. An open crack filled with air has very low acoustic impedance, so it reflects virtually all the acoustic energy incident on it, as presented in Figure 4. Hence, the sound waves travel through the material and are reflected back from cracks or flaws. Defects and flaws affect its path, and a small portion of the pulse will be sent back to the transducer/receiver before it hits the boundary of the structure. The reliability of sonic data is largely determined by the skill and experience of the operator in choosing appropriate test points and in observing those conditions that might influence the measurements. Such factors as changes in density, moisture, aggregate-paste ratio, and the presence of voids and cracks should all be given weight in the final analysis.

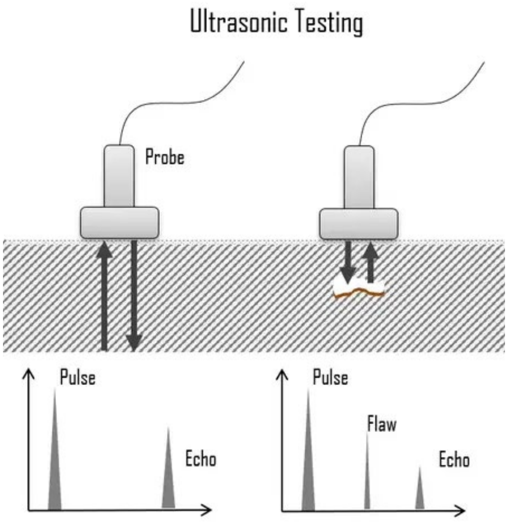

Figure 4 – Schematic diagram of the ultrasonic testing.

Modern UPE instruments consist of an array of piezoelectric transducers that are capable of exciting concrete surface by a short-burst high amplitude pulse with -high voltage and high current. MIRA (owned by the measurement operator "Kiwa Inspecta, Finland"), presented in Figure 5, is an ultrasonic tomography device that "can be used to diagnose condition of inner parts of a concrete structure using an array of dry point contact (DPC) transducers. Each transducer can both transmit and receive low frequency (55 kHz) shear waves.

Figure 5 – Example of a UPE system, array of transducers and measurement images [12].

The DPC transducers provide the necessary consistency of impact and wavefront penetration for diagnostics up to 100 cm deep for typical concrete surface textures. MIRA incorporates 12 channels each comprised of 4 transducers in a multi-static array. After transit time data are acquired at a test location, a signal processing technique called Synthetic Aperture Focusing

Technique (SAFT, owned by Kiwa Inspecta, Finland) is used to reconstruct a 2-D image of the interior of the concrete member at the test location [11].

2 EXPERIMENTAL PROGRAM

2.1 Mock-up wall reinforcement design

The design for the mock-up wall was based on the section of the containment wall of TVO's NPP Olkiluoto 2 [13]. This mock-up wall of reinforced concrete presented in Figure 7 is 1.0 m thick, 2.0 m high, and its length is 3.5 m [14].

Figure 6 – Mock-up wall on its foundation [14].

The mix design of the concrete was based on the C35/45 compressive strength class and S3 consistency class. A total of two truck batches were needed for its casting. The mix design was the same on both batches and average amounts of the realized constituents are shown in Table 1.

Table 1 – Mix design of C35/45 concretes – provided from the ready-mix concrete plant.

Concrete mix		Concrete ingredients (kg/m³)	Aggregates free moisture (%)	Aggregates free moisture (kg/m³)
Cement (CEM II/B-M (S-LL) 42,5 N)		365.5		
Aggregates	(0/8 mm)	1044.9	1.3	16.6
	(8/16 mm)	901.8	0.6	5.4
Water	Hot water	49.8		
	Cold water	102.3		
Effective water content		174,1		
Super-plasticizer (Master Glenium SKY 600)		2.74		

Fresh concrete tests were performed during the casting prosess and three cubes (100 × 100 × 100 mm) were prepared for testing the compresive strenght at ages of 28 and 91 days. The test results of the fresh and hardened concrete are presented in Table 2.

Table 2 – Summary of the fresh and hardened concrete test results.

Property of concrete	Unit	Batch I	Batch II
Temperature	[°C]	21	20
Slump	[mm]	170	180
Air content	[%]	3.7	1.0
28d Compressive strength	[MPa]	43	44
91d Compressive strength	[MPa]	51	52

The reinforcement of the wall consists of two areas, with different spacing between bars, which led to different amounts of reinforcement for these areas. The bar diameter used is 25 mm. The nominal reinforcement concrete cover is 50 mm [15]. The outer layer of reinforcement is characterized by a reinforcement grid with the following characteristics: the left half side of the mock-up when facing the wall consists of horizontal reinforcement with a spacing of 150 mm and vertical reinforcement with a spacing of 150 mm. The right half side includes horizontal reinforcement with a spacing of 300 mm and vertical reinforcement with a spacing of 200 mm (Figure 7).

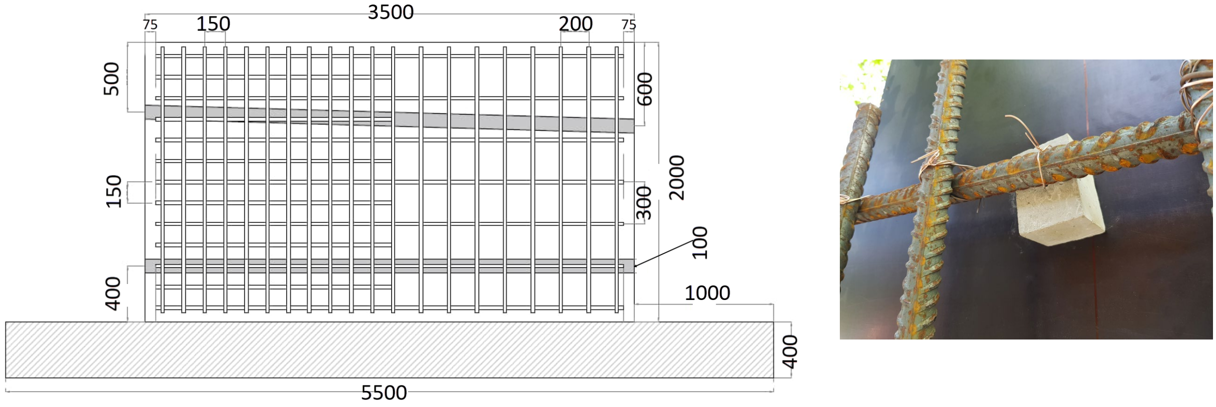

(a) (b)

Figure 7 – (a) Frontal view of the mock-up wall with its reinforcement and (b) embedded 50 mm concrete block for indicating the actual cover thickness of the reinforcement bars.

As shown in Figure 7a, the second reinforcement mesh exists only on the left side of the mock-up in the frontal view. This reinforcement mesh has horizontal and vertical reinforcements with a spacing of 150 mm. Additionally, some bars were installed at an angle, and in some places, single rebars were installed outside other reinforcements. The rebars on the south face of the wall have inconsistent average spacing. The horizontal reinforcement bars of the wall were adjusted to ensure the concrete covering requirements before concreting. Concrete blocks of 50mm thickness were used to maintain the required concrete cover depth (Figure 7b).

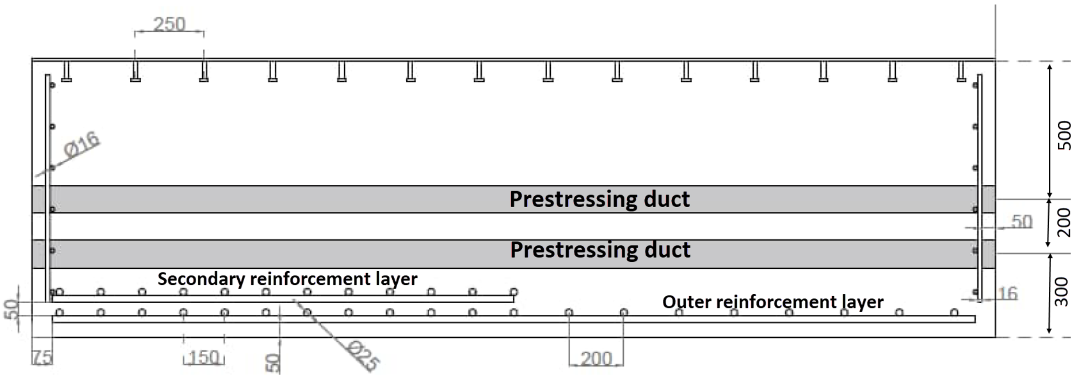

Figure 8 – Plan view of the mock-up main wall reinforcement.

Three ducts for pre-stressed tendons and corresponding strands were inserted into the mock-up wall. The tendon ducts were located at two heights in the wall, as well as at two different depths from the outer surface. One duct was placed behind another, simulating the use of parallel ducts at same height, which is a common situation in Nuclear Power Plant containment structures. Figure 9 illustrates the locations of the ducts from the side view.

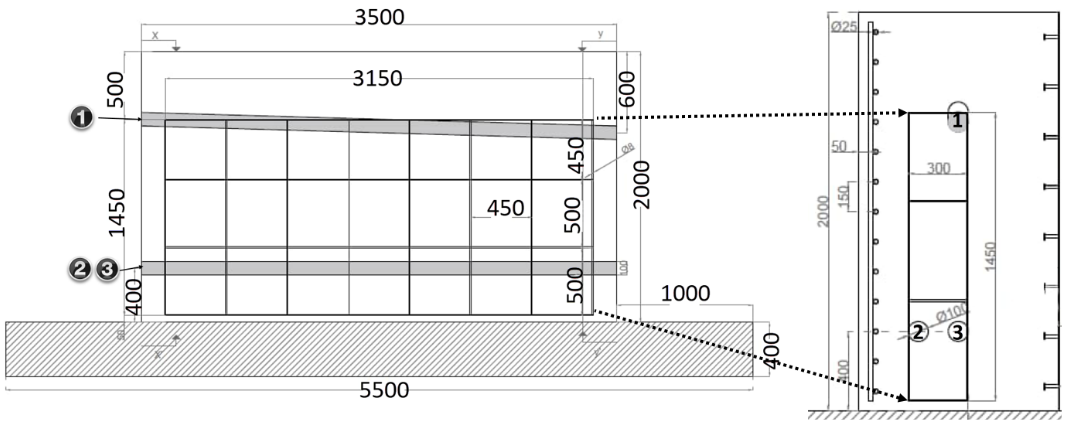

Figure 9 – Location of the pre-stressed tendon ducts, side views.

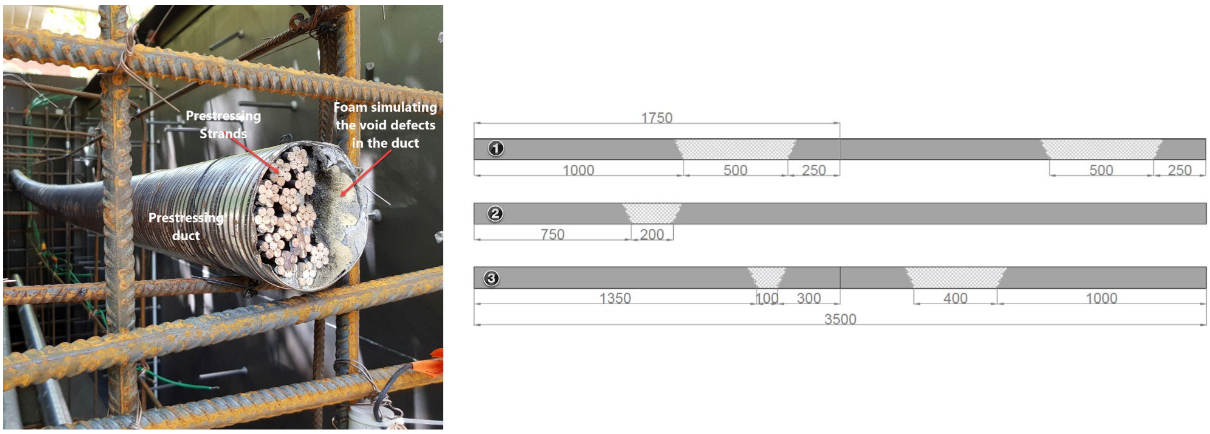

Figure 10 – Location of the void defects in the pre-stressed tendon ducts.

The injection grouting of the duct was planned not to fil the entire space leaving air filled parts in the duct to be investigated using NDT methods (Figure 10). A void-existed defects induced by the interface debonding between the grouting medium and duct's inner surface due to the initial void in grouting medium within the duct of post-tensioned concrete members, specimens with void defect in grouting medium was formed by presetting a foam in the duct.

2.2 Measuring the thickness of concrete cover

For measuring the concrete cover, the cover meter method was used. The cover meter was calibrated using the calibration test block, presented in Figure 11. The location and cover of the reinforcement of the test block were measured at different locations to check the calibration accuracy of the device. The calibration measurement data were compared with the standard values prescribed for the test block. The measured data and the standard calibration values matched well.

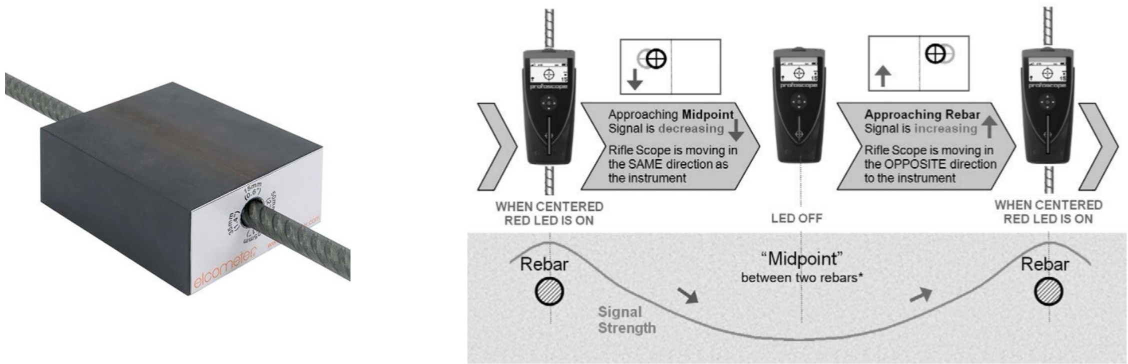

(a) (b)

Figure 11 – Concrete cover meter: (a) the calibration test block and (b) distinguishing between a rebar and a mid-point using cover meter [16].

The cover meter was used to measure the cover from the south side of the mock-up wall in the horizontal and vertical direction. As soon as the cover meter was above or near a rebar, it gave an audio signal through a short beep and a visual red colour display. Simultaneously, the thickness of concrete cover was measured and recorded. To ensure that the positioning of the probe at the moment of the signal, the probe was continuously dragged along the wall surface.

2.3 Mapping of the reinforcement meshes and bars

For mapping and locating the positions of the reinforcement in the mock-up wall, two radar-based GPR devices (GPR1 and GPR2) and an ultrasonic-based UPE tomography device were used.

In addition to mapping the positions of the reinforcement, the condition of tendon strands was examined using a device based on UPE tomography. The inspections were performed on the southern concrete-surfaces of the mock-up wall. Scans with UPE device were performed in two directions similar to that presented in Figure 12. The extent of the areas inspected was partly influenced by the spatial requirements of the devices.

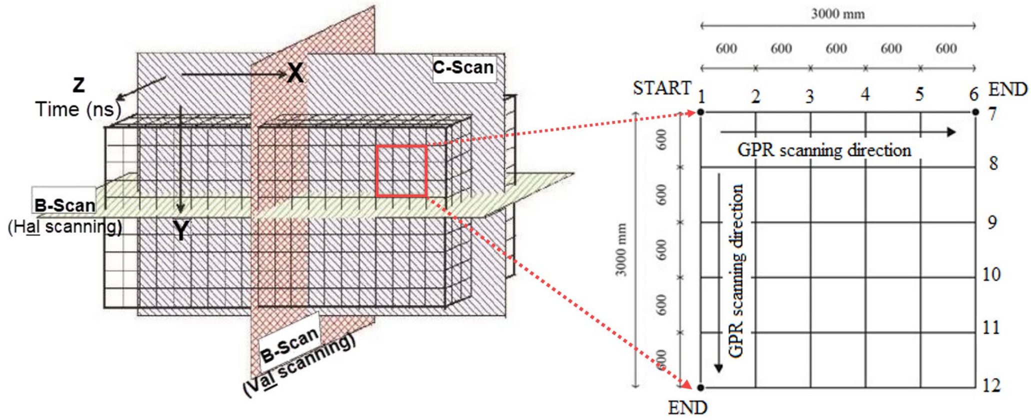

Figure 12 – Illustration of the grid mark scheme of the mock-up wall and the scanning direction.

3. RESULTS AND DISCUSSION

3.1 Concrete cover depth measurements

For the horizontal reinforcement bars, the cover meter was set to identify a clear cover of 50 mm above steel bars with a diameter of 25 mm. As shown in Figure 13, the thickness of concrete cover varies from 39 mm to 51 mm. The mean of the thickness values measured is 44 mm, and the standard deviation is 1.7 mm leading to the coefficient of variation of 3.8%. The results show that the cover thickness differs about 10% from the design value 50 mm.

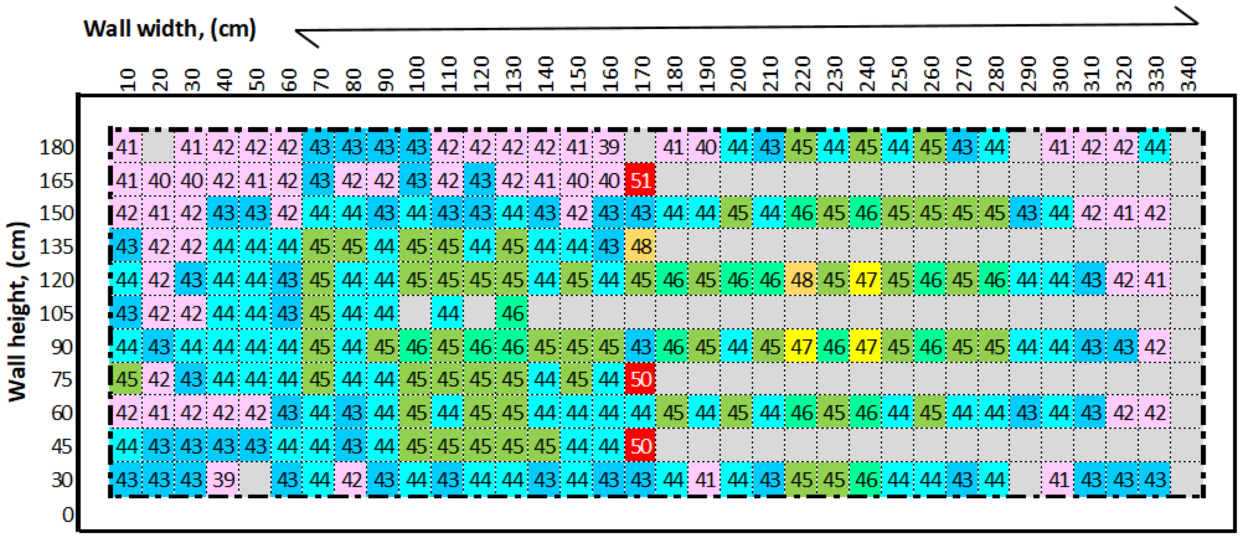

Figure 13 – Concrete cover thickness scanned for horizontal reinforcement on the south face of the wall).

For the vertical reinforcement bars, the cover meter was set to identify a clear cover of 75 mm on steel bars with a diameter of 25 mm. The results presented in Figure 14 show that the concrete cover varies from 49 mm to 77 mm. The mean of the concrete cover thickness is 60 mm, and the standard deviation is 5.8 mm, or the coefficient of variation is 9.7%. As the design value for the concrete cover of vertical bars was 75 mm, the difference between the measured and design values is about 25%, which is larger than the difference with horizontal bars. This is obviously a consequence of the shadow effect of the horizontal bars on the scanning of vertical bars. The shadowing also explains why the cover thickness of the second mesh with design cover values of 100 mm for horizontal bars and 125 mm for vertical bars could not be detected using the cover meter.

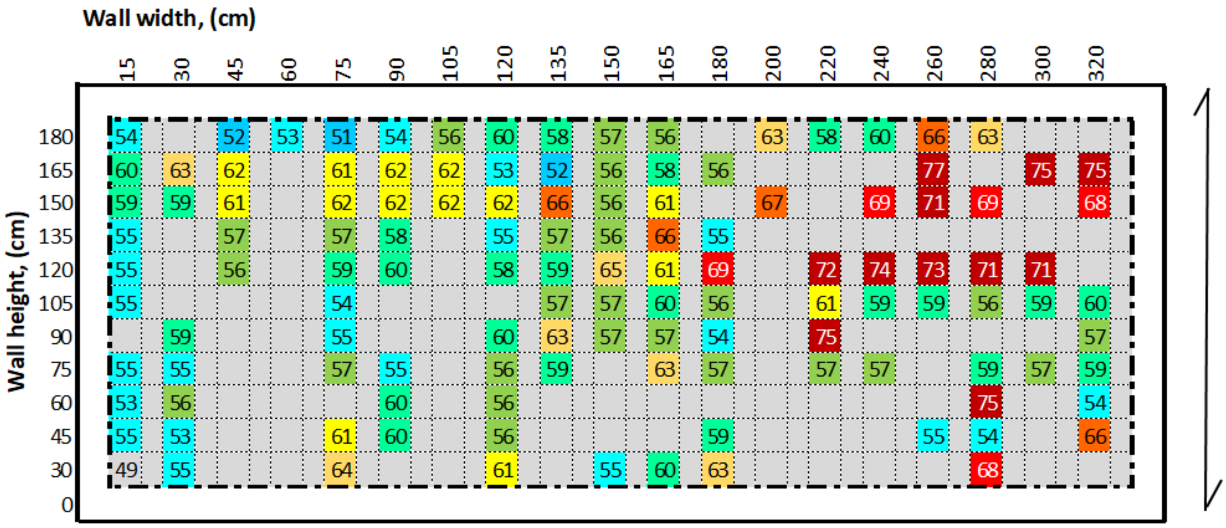

Figure 14 – Concrete cover depth (south face, vertical reinforcement scanning).

Table 3 shows the results of the detected cover for the south face of the reinforced concrete mock-wall. The data in the table show that cover meter can effectively be used to measure the cover depths. The relative error in detection of the cover depth increases in the left half face where higher reinforcement density is located.

Table 3 – Details of the detected clear cover depth for both horizontal and vertical reinforcement scanning.

Reinforcement	Average detected cover, (mm)	Actual location of bar from top surface, (mm)	Accuracy (Relative error), (%)	Standard deviation, (mm)	Coefficient of variation, (%)
Horizontal bars	44	50	-12%	1.7	3.8
Vertical bars	60	75	-20%	5.8	9.7

3.2 Mapping of the reinforcement steel bars

The scanning results of the southern face of the mock-up wall using the GPR1 device are presented in Figures 15 and 16. Figure 15 presents the acquired 3D radargram of southern part of the mock-up wall after data processing, and Figure 16 shows the C-scan image (see Figure 12) of the same wall face.

The 3D radargram and the C-scan images show the dense reinforcement with bar spacings of 150 mm on the left part of the wall and the mesh with bar spacings of 300 mm on the right half of the wall face. The second mesh was shown on the left of the 3D radargram, but no details were recognized.

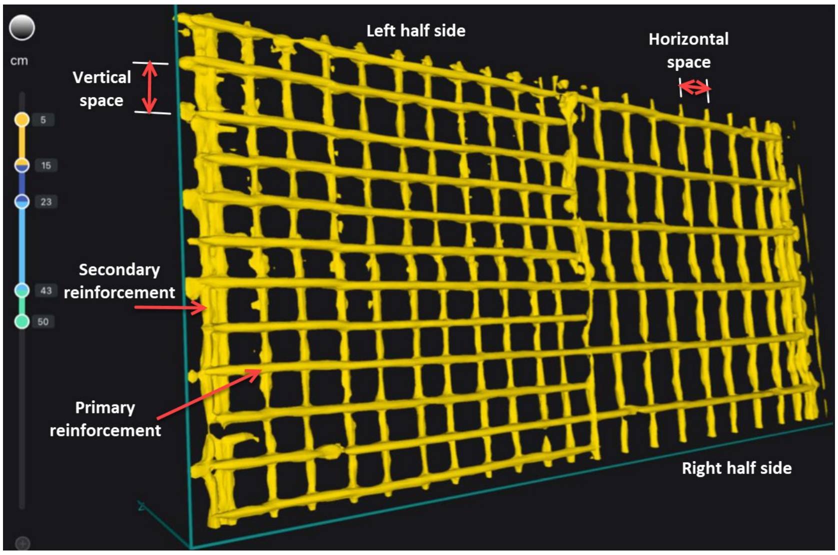

,

Figure 15 – Representation of the near-surface reinforcement of the southern face using GPR1 device.

Figure 16 also includes a lower prestressing duct and the edges of the second mesh in the middle and on the left of the wall face. However, no clear details about the second mesh are visible, which can be explained by the shadowing effect of the first mesh.

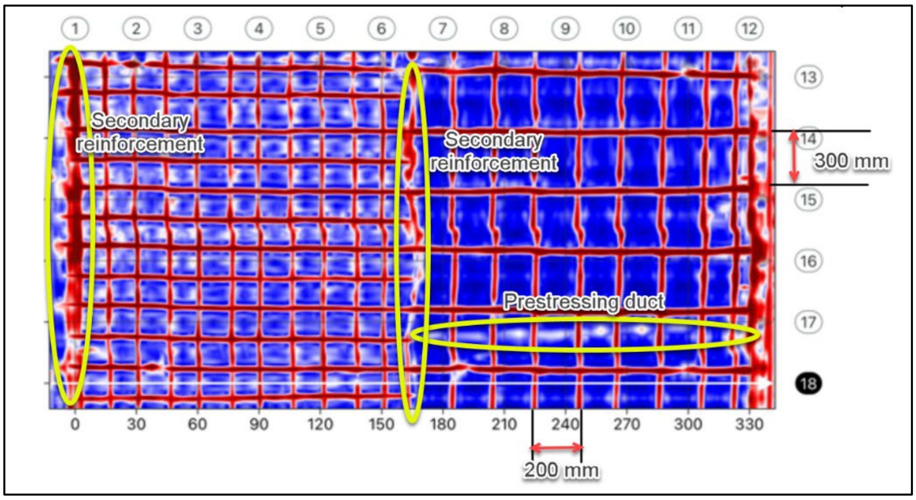

Figure 16 – C-Scan of the near-surface reinforcement of the southern side using GPR1 device.

Figures 17 and 18 present the Augmented Reality (AR) view and the C-scan view of the pre-stressing duct at depth of 52 cm from the surface using GPR1 device. In Figure 17, the location of a lower pre-stressing duct is clearly shown, but the location of the upper duct is open to interpretation because the depth of the scanning presented in Figure 18 is 29 - 52 cm and the upper duct is located behind this depth. The empty spaces in the injection grouting of the space were detected at the lower prestressing duct as shown in Figure 18.

Figure 17 – Visual representation of the tendon strand on the southern side as an Augmented Reality (AR) view on the surface of the real structure using GPR1 device.

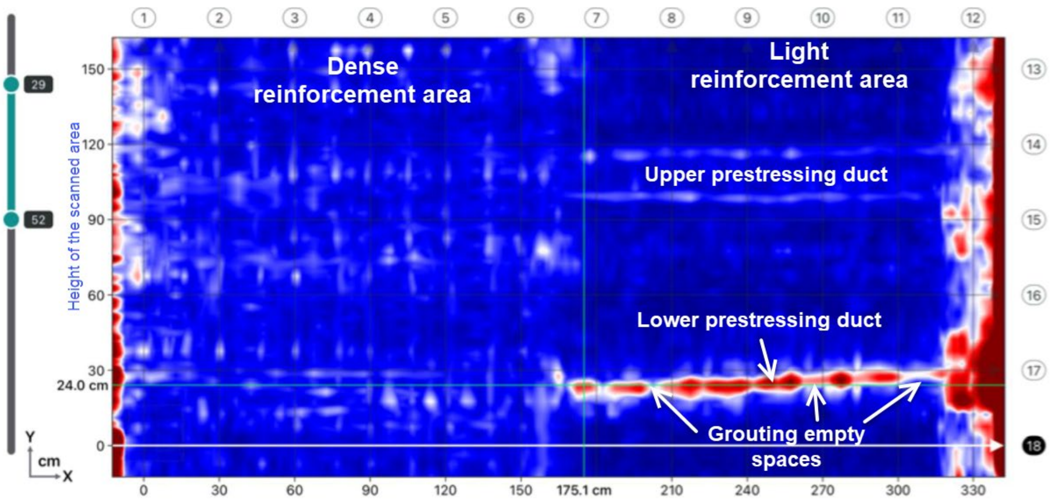

Figure 18 – Visual representation (C-Scan) of the tendon strand on the southern side using GPR1 device at the depth of 29 - 52 cm from the surface, compared to Figure 15.

An example of the C-scan image after the data processing of the GPR2 device is presented in Figure 19. The origin is located 175 mm from the bottom edge and 1315 mm from the left edge.

On average the spacing of the horizontal and vertical rebars on the left side in the figure is 150 mm as the design values were. On the right side, the average spacing of the horizontal and vertical bars and the design values also match. Figure 19 also shows that the concrete cover thickness on the top of the horizontal bars is about 50 mm and about 75 mm on the top of the vertical bars, which coincide with the design values presented in Figure 7.

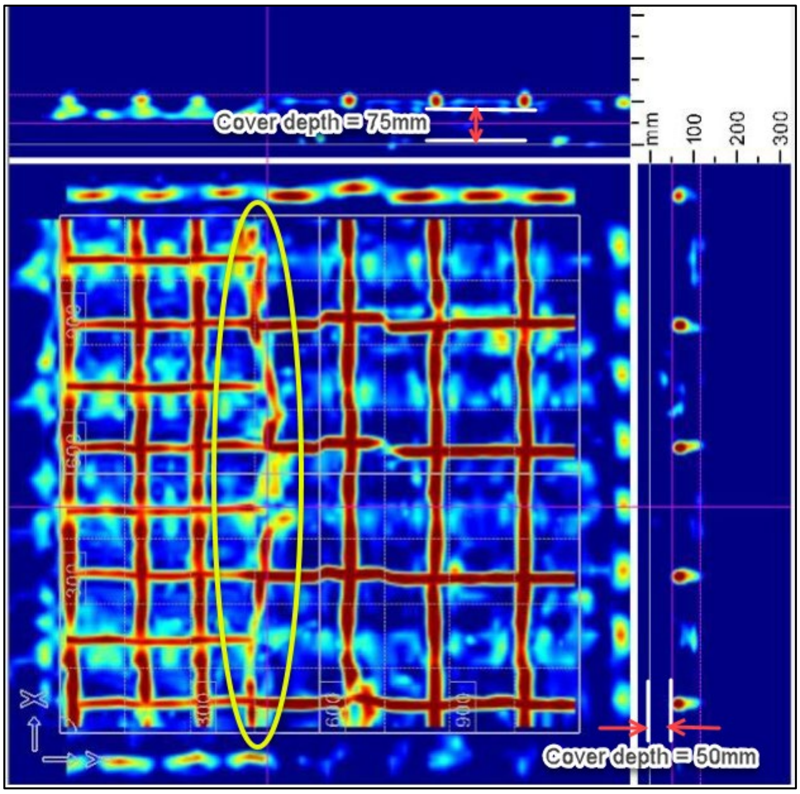

Figure 19 – Representation of the vertical middle part of the southern side using GPR2 device.

3.3 Condition monitoring of prestressing tendon ducts

Ultrasound tomography is probably the most suitable NDT technique to evaluate the outcome of grout injection of ducts with prestressed tendons. The ultrasound "MIRA" tomographer system was used in this study to perform deep scanning from one surface of the concrete structure and data processing of the scanning results. The MIRA tomographer creates 3D representation of internal reflecting interfaces (e.g., defects) that may be present in a concrete structure.

Based on the visual observations from the UPE scan, the injection grouting of the duct tube of the tendon strand is incomplete, which is shown in Figures 20 and 21. The depth of the UPE scanning is 50 cm from the surface of the southern face of the mock-up wall. The location of the prestressing duct is about 50 cm (design value of 40 cm) from the slab foundation as shown in Figure 20. The upper duct tube is inclined as shown in the C-scan of Figure 21, the right side of the duct is located at about 130 cm (design value of 140 cm) from the foundation slab and the left side of the duct is located at about 140 cm (design value of 150 cm) from the foundation slab. The observed UPE values are higher in comparison to the design values, which could be due to the movement of the duct during the installation and casting of the concrete.

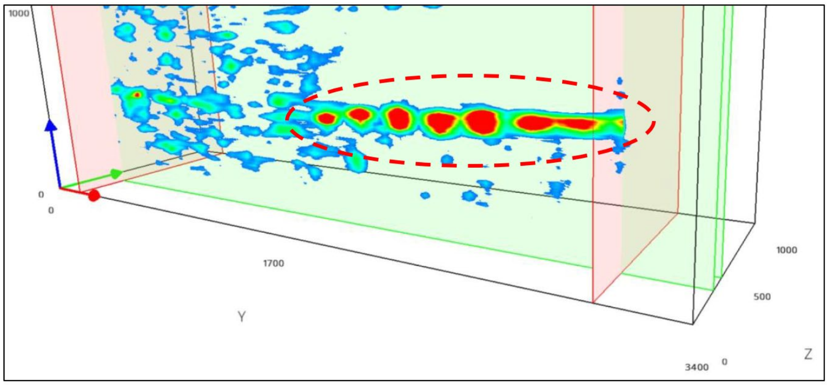

Figure 20 – Visual representation of the lower tendon strand using the UPE device.

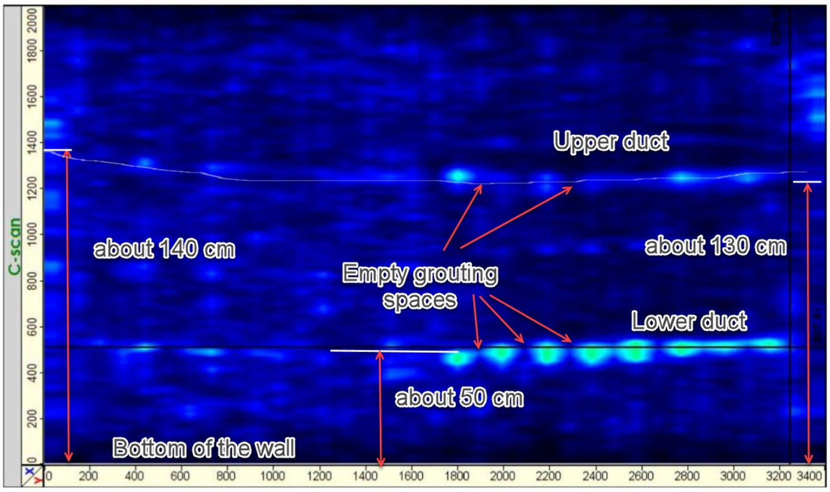

Figure 21 – Visual representation of the tendon strand using the UPE device compared to Figure 18.

4 CONCLUSIONS

In this paper, we presented three different techniques for detecting, and mapping of the steel reinforcement bars in a thick mock-up wall of reinforced concrete The three NDT techniques were electromagnetic methods using concrete cover meter, ground penetrating radar (GPR) and ultrasonic pulse echo (UPE), which were used to scan the southern face of the mock-up wall horizontally and vertically to detect reinforcement in the structure.

The following conclusions can be drawn from the results of the study:

- Cover meter and GPR techniques can be used for steel bar identification and cover thickness estimation. In general, the cover meter technique is simple to use, and its results are easy to interpret compared to that of GPR technique. The concrete cover thicknesses measured by the cover meter were close to the real values.
- By using real bar diameters during the calibration of the cover meter, the results of the cover thickness are reliable.

- Structural members with thick concrete covers and heavily reinforced sections with metal inserts, identification of reinforcement using cover meter is difficult. In such cases, GPR technique is better in identifying the locations of steel bars and estimating cover thicknesses.
- The GPR technique is able to locate and map the reinforcement bars via the 3D radargram and the C-scan images. One of the limitations of the GPR techniques is that it needs an experienced technician for the use of the scanner and interpretation of the results. Another limitation is that the radar pulse penetration depth with the GPR system used was limited to approximately 30 cm.
- Evaluation of tendon duct grout injection by applying UPE technique is proven to be beneficial in detecting substantial durability problems that may pose risks to the prestressing system. For example, the UPE devices can detect the prestressing duct with insufficient grouting. The interpretating tomography testing results should have an appropriate understanding and experience in performing these types of tasks.

ACKNOWLEDGEMENTS

The authors would like to thank the following people who have helped us undertake this research: Jukka Hietikko, Sami Kallio, Olli Pelkonen and Tuure Junkkari from Kiwa Inspecta (Finland) for their performing of the NDT measurements using GPR and UPE devices and reporting the scanning.

REFERENCES

1. Frankowski P & Chady T: "Impact of Magnetization on the Evaluation of Reinforced Concrete Structures Using DC Magnetic Methods". 2022, doi: 10.3390/ma15030857.
2. Hüblová S, Cikrle P, Karel O & Kocáb D: "Experimental measurement of the diameter and cover depth of steel reinforcement using an electromagnetic concrete cover meter". *Proceedings*, IOP Conf Ser Mater Sci Eng, Vol. 549, No. 1, p. 012011, Jun. 2019, doi: 10.1088/1757-899X/549/1/012011.
3. Raupach M & Büttner T: "Concrete Repair to EN 1504 Diagnosis, Design, Principles and Practice". *CRC Press*, London, UK, 2014. doi: 10.1201/b16852.
4. Balayssac J P & Garnier V: "Non-destructive Testing and Evaluation of Civil Engineering Structures". *Elsevier Inc*., 2017. doi: 10.1016/C2016-0-01227-5.
5. Tosti F & Ferrante C: "Using Ground Penetrating Radar Methods to Investigate Reinforced Concrete Structures". *Surv Geophys*, Vol. 41, No. 3, pp. 485–530, May 2020, doi: 10.1007/S10712-019-09565-5.
6. Wiwatrojanagul P, Sahamitmongkol R, Tangtermsirikul S & Khamsemanan N: "A new method to determine locations of rebars and estimate cover thickness of RC structures using GPR data". *Construction Building Materials*, Vol. 140, pp. 257–273, June 2017, doi: 10.1016/J.CONBUILDMAT.2017.02.126.

7. Luo T, Lai W, Chang R & Goodman D: “GPR imaging criteria”. *Journal of Applied Geophysics*, Vol. 165, pp. 37–48, Jun. 2019, doi: 10.1016/J.JAPPGEO.2019.04.008.
8. Merkle D, Frey C & Reiterer A: “Fusion of ground penetrating radar and laser scanning for infrastructure mapping”. *Journal of Applied Geodesy*, Vol. 15, No. 1, pp. 31–45, Jan. 2021, doi: 10.1515/JAG-2020-0004/MACHINEREADABLECITATION/RIS.
9. Sbartaï M, Laurens S, Rhazi J, Balayssac J P & Arliguie G: “Using radar direct wave for concrete condition assessment: Correlation with electrical resistivity”. *J Appl Geophy*, Vol. 62, No. 4, pp. 361–374, Aug. 2007, doi: 10.1016/J.JAPPGEO.2007.02.003.
10. Krause M & Wiggenhauser H: “Ultrasonic pulse echo technique for concrete elements using synthetic aperture”. Proceedings, International Conference on NDT in Civil Engineering, 8-11 April 1997, the University of Liverpool, British Institute of Non-Destructive Testing, 1997, p. 806.
11. Kwon H, Joh C & Chin W J: “3D Internal Visualization of Concrete Structure Using Multifaceted Data for Ultrasonic Array Pulse-Echo Tomography”. *Sensors,* Vol. 21, No. 19, p. 6681, Oct. 2021, doi: 10.3390/S21196681.
12. Bishko A V, Samokrutov A A & Shevaldykin V G: “Ultrasonic echo-pulse tomography of concrete using shear waves low-frequency phased antenna arrays”. *Proceedings*, 17th World Conference on Nondestructive Testing, 25-28 Oct 2008, Shanghai, China, 2008, pp. 25–28. Accessed: Sep. 20, 2023. [Online]. Available: https://www.ndt.net/?id=6362
13. Teollisuuden Voima - TVO Oyj, “Nuclear power plant units Olkiluoto 1 and Olkiluoto 2 (OL1 and OL2).” Accessed: Sep. 20, 2023. [Online]. Available: https://www.tvo.fi/en/index/production/plantunits/ol1andol2.html
14. Al-Neshawy F, Ferreira M, Bohner E, Ojala T, Sjöblom V, Niederleithinger E, Effner U & Puttonen J: “Design, construction, and NDT of a mock-up for reinforced concrete walls in NPP”. in International Conference on Structural Mechanics in Reactor Technology, SMiRT 25 - Charlotte, United States, Charlotte, 2019, p. 12. Available: https://repository.lib.ncsu.edu/bitstream/handle/1840.20/37937/VIII_667_Fahim_Al_Neshawy.pdf?sequence=1
15. Al-Neshawy F, Ferreira M & Puttonen J: “Combined NDT methods to determine the variations in compressive strength throughout concrete structures”. *Proceedings*, International Conference on Non-destructive Evaluation of Concrete in Nuclear Applications - NDE NucCon 2023, pp. 368–376, 2023, Accessed: Sep. 20, 2023. [Online]. Available: https://research.aalto.fi/en/publications/combined-ndt-methods-to-determine-the-variations-in-compressive-s
16. Proceq, “Profoscope operating instructions”. 2017. Accessed: Sep. 21, 2023. [Online]. Available: https://media.screeningeagle.com/asset/Downloads/Profoscope_Operating%20Instructions_English_high.pdf